Molecular Neurobiology (2019) 56:1933–1945
https://doi.org/10.1007/s12035-018-1217-3

Spatial Distribution and Expression of Ectonucleotidases in Rat Hippocampus After Removal of Ovaries and Estradiol Replacement

Ivana Grković[1] · Nataša Mitrović[1] · Milorad Dragić[1,2] · Marija Adžić[2] · Dunja Drakulić[1] · Nadežda Nedeljković[2]

Received: 13 April 2018 / Accepted: 29 June 2018 / Published online: 6 July 2018

Abstract

Purinergic signaling is the main synaptic and non-synaptic signaling system in brain. ATP acts as a fast excitatory transmitter, while adenosine sets a global inhibitory tone within hippocampal neuronal networks. ATP and adenosine are interconnected by ectonucleotidase enzymes, which convert ATP to adenosine. Existing data point to the converging roles of ovarian steroids and purinergic signaling in synapse formation and refinement and synapse activity in the hippocampus. Therefore, in the present study, we have used enzyme histochemistry and expression analysis to obtain data on spatial distribution and expression of ecto-enzymes NTPDase1, NTPDase2, and ecto-5′-nucleotidase (eN) after removal of ovaries (OVX) and estradiol replacement (E2) in female rat hippocampus. The results show that target ectonucleotidases are predominantly localized in synapse-rich hippocampal layers. The most represented NTPDase in the hippocampal tissue is NTPDase2, being at the same time the mostly affected ectonucleotidase by OVX and E2. Specifically, OVX decreases the expression of NTPDase2 and eN, whereas E2 restores their expression to control level. Impact of OVX and E2 on ectonucleotidase expression was also examined in purified synaptosome (SYN) and gliosome (GLIO) fractions. Data reveal that SYN expresses NTPDase1 and NTPDase2, both of which are reduced following OVX and restored with E2. GLIO exhibits NTPDase2-mediated ATP hydrolysis, which falls in OVX, and recovers by E2. These changes in the activity occur without parallel changes in NTPDase2-protein abundance. The same holds for eN. The lack of correlation between NTPDase2 and eN activities and their respective protein abundances suggest a non-genomic mode of E2 action, which is studied further in primary astrocyte culture. Since ovarian steroids shape hippocampal synaptic networks and regulate ectonucleotidase activities, it is possible that cognitive deficits seen after ovary removal may arise from the loss of E2 modulatory actions on ectonucleotidase expression in the hippocampus.

Keywords Ectonucleotidases · Hippocampus · Ovariectomy · Estradiol · Astrocytes

Introduction

Besides their well-known role(s) in the regulation of the reproductive system, fluctuations of estrogens and progestins during menstrual (or estrous) cycle induce fine ultrastructural and functional alterations in select brain regions, including the hippocampus [1, 2]. Since the first report of Woolley and McEwen in 1993, that spine density of pyramidal neurons in the hippocampal CA1 field correlates with estrogen levels during the estrous cycle [3], numerous studies using the classic endocrine paradigm of ovariectomy (OVX) and estradiol replacement repeatedly confirmed its neurotrophic effects and induction of synapse formation and maturation in several species, including mouse, rat, and rhesus monkey [1, 4–10]. At functional level, estradiol has been shown to improve performance in hippocampus-dependent spatial memory tests in rodents [7–9, 11] and cognitive tests after surgically induced menopause in human subjects [12, 13]. Besides neurons, glial cells express estradiol receptors (ER) and respond to estradiol action [14]. For instance, estradiol inhibits phagocytosis and attenuates pro-inflammatory responses in microglia [14, 15].

Electronic supplementary material The online version of this article (https://doi.org/10.1007/s12035-018-1217-3) contains supplementary material, which is available to authorized users.

✉ Ivana Grković
istanojevic@vin.bg.ac.rs

[1] Department of Molecular Biology and Endocrinology, Vinča Institute of Nuclear Sciences, University of Belgrade, Mike Petrovića Alasa 12-14, Belgrade 11001, Serbia

[2] Department for General Physiology and Biophysics, Faculty of Biology, University of Belgrade, Studentski trg 3, Belgrade 11001, Serbia

The hormone also regulate the functions of astrocytes and their communication with other cell types in the central nervous system (CNS), while under pathological conditions, astrocytes mediate, at least partially, the neuroprotective effects of ovarian hormones (for review see [16]). Thus, estradiol activates many mechanisms in neurons and glial cells which maintain homeostasis and promote neuroprotection [16–20]. It is not surprising that a decline in the endocrine function of ovaries and the resulting decrease in circulating estradiol levels during physiological or surgically induced menopause affect the brain, among other target organs. Epidemiological data show that menopause is associated with a considerable degree of cognitive impairment [21], and at least, a part of the deficits may arise from the lack of estradiol and its modulatory actions in the hippocampus [22].

Extracellular purine nucleotide ATP and nucleoside adenosine are yet other important modulators of hippocampal function and plasticity. Extracellular ATP plays an important role in neuron-glial communication and interactions between different transmitter systems, by acting at subsets of P2 receptors [23–25]. Adenosine, which operates via P1 receptor subtypes, is a neuromodulator involved in fine-tuning of neurotransmission with a strong impact on synaptic plasticity and learning [26]. The levels of ATP and adenosine in the extracellular space are tightly regulated by the coordinated action of ectonucleotidase enzymes, expressed at the outer membrane surface in different cell types in the CNS [27]. The enzymes catalyze the sequential hydrolysis of ATP to adenosine, thus suspending signaling actions of ATP and promoting adenosine signaling via P1 receptors [23, 27]. Ectonucleotidases comprise several families of nucleotide-metabolizing enzymes, including ecto-nucleoside triphosphate diphosphohydrolase1-3 (E-NTPDase1-3) and ecto-5′-nucleotidase (eN/CD73) [27, 28]. NTPDase1 (CD39) hydrolyzes ATP and ADP equally well to AMP, whereas NTPDase2 and NTPDase3 show much higher affinity for ATP, thus leading to a transient accumulation of ADP in the pericellular space [27, 28]. The final and the rate-limiting step in the extracellular ATP degradation is catalyzed by ecto-5′-nucleotidase, which converts AMP to adenosine [27].

The ectonucleotidase enzymes have distinct and mutually overlapping regional and cellular distribution in the brain [27–30]. Thus, NTPDase1 is mainly associated with microglia, vascular endothelium, and neurons [29, 31–33], while NTPDase2 is localized at astrocytes [34–37] and astrocyte-like progenitor cells of the subventricular zone [37, 38]. NTPDase3 is restricted to neurons in the midline thalamic and hypothalamic nuclei, with low level being expressed in the hippocampus [39, 40]. Ecto-5′-nucleotidase is widely associated with neurons, microglia, astrocytes [29–31, 41]. In addition, the whole enzyme chain, i.e., NTPDase1/NTPDase2/NTPDase3/eN has been demonstrated in synaptic compartments isolated from different brain regions, including the hippocampus [29, 32, 40, 42–47].

The extracellular purine nucleotide metabolism and particularly the activity of eN are under the complex control by ovarian steroids. Thus, recurring fluctuations in eN activity in rat hippocampal synaptic membranes have been observed across the 5-day estrous cycle [47]. It is of note that the changes in eN activity were not always correlated with the eN gene and/or protein expression [44, 46–49], implying that ovarian steroids may regulate eN at transcriptional, as well as post-translational level. Thus, single dose [47] or multi-dose of estradiol [50] administered to OVX rats, strongly upregulated eN expression and increased enzymatic efficiency in hippocampal synaptic membranes, through the mechanism(s) which engaged both ERα and ERβ [47]. Studies regarding the role of ovarian steroids in the regulation of other members of ectonucleotidase family are scarce.

Given that the ectonucleotidases have distinct and overlapping distribution in rat hippocampus [29–31], and that the enzymes and the ovarian hormones participate in a formation, maturation, and a refinement of synaptic contacts, both during development and in adulthood [1, 4–10, 30], the aim of the present study was to obtain data on spatial distribution and cellular targets of estradiol-induced effects on ectonucleotidases in rat hippocampus. To this end, alterations in ectonucleotidase activities following OVX and estradiol treatment (E2) were visualized by enzyme histochemistry, which provided a link between a function and spatial localization of individual ectonucleotidase, and the data were compared with conventional mRNA, protein, and functional analyses conducted in two distinct subcellular membrane fractions, synaptosomes and gliosomes which are enriched in synaptic and glial membranes, respectively. The effects obtained in gliosome fraction were further explored in primary hippocampal astrocyte culture.

Material and Methods

Chemicals

Analytical grade salts and buffer reagents, 17β-estradiol 3-benzoate (E2), adenosine 5′-triphosphate disodium salt hydrate (ATP), adenosine 5′-diphosphate sodium salt hydrate (ADP), adenosine 5′-monophosphate sodium salt hydrate (AMP), levamisole hydrochloride, Percoll®, dimethyl sulfoxide (DMSO), bovine serum albumin (BSA), and paraformaldehyde (PFA) were purchased from Sigma-Aldrich (St. Louis, MO, USA). Leibovitz's L-15 Medium, Penicillin/Streptomycin, Fetal Bovine serum (FBS), and Dulbecco's modified Eagle's medium (DMEM) were obtained from Gibco (ThermoFisher Scientific, Waltham, MA, USA).

Animals

All experiments were conducted on 10-week-old female Wistar rats (200–250 g) obtained from local colony. Appropriate actions were taken to alleviate the pain and discomfort of the animals in accordance with the compliance with European Communities Council Directive (2010/63/EU) for animal experiment, and the research procedures were approved by the Ethical Committee for the Use of Laboratory Animals of Vinča Institute of Nuclear Sciences, University of Belgrade, Republic of Serbia (Application No. 02/11). Animals were housed (3–4/cage) under standard conditions: 12-h light/dark regime, constant ambient temperature (22 ± 2 °C), and free access to food and water.

Estrus Cycle and Treatment

Total of 20 female rats was used to assess the fluctuation in the estrous cycle. The estrous cycle stages were monitored between 9 and 10 am during 2 weeks, and only the animals with regular 4–5-day cycle were included in experiments. Rats were assigned to one of the three estrous stages: proestrus, estrus, and diestrus according to relative proportion of epithelial-nucleated cells, squamous cells, and leukocytes in vaginal smears. Since our previous report [47] has shown great differences in the eN activity between diestrus and OVX females, the animals in diestrus were mobilized in the group of intact control (Int). Another group of females (n = 48) was subjected to a bilateral removal of ovaries (OVX), through one dorsal incision. The surgery was conducted under ketamine (50 mg/kg) s.c. and xylazine (5 mg/kg) s.c. anesthesia. Three weeks after the removal of ovaries, animals were randomly divided into three groups (16 rats/group) and treated s.c. as follows: (1) the OVX group, without further treatment; (2) OVX group which received an injection of DMSO (1 ml/kg); (3) OVX rats injected with one dose of 17β-estradiol benzoate (33.3 μg/kg; OVX + E2). The same dose of E2 was used in the previous studies [46, 47, 50] and produces supraphysiological estradiol levels in circulation of ovariectomized females shortly after injection, which is metabolized to physiological level within 24 h [3]. The E2 was applied in the morning (9:00 am) and animals were sacrificed after 24 h.

Enzyme Histochemistry

For enzyme histochemistry, the brain was carefully removed from a skull and fixed in 4% paraformaldehyde/0.1 M phosphate buffer (pH 7.4). After cryoprotection in graded sucrose solutions (10–30% in 0.2 M phosphate buffer) at 4 °C, 20-μm-thick brain sections were mounted on gelatin-coated slides, dried for about 2 h at room temperature, and stored at − 20 °C until use. ATPase and AMPase enzyme histochemistry were performed as described previously [29, 45]. Briefly, cryosections were preincubated for 30 min at room temperature with TRIS-maleate sucrose (TMS) buffer containing 0.25 M sucrose, 50 mM TRIS-maleate, 2 mM levamisole, and 2 mM $MgCl_2$ (pH 7.4). The enzyme reaction was performed at 37 °C in a TMS-buffered substrate solution for 60 min, containing ATP, ADP, or AMP in 1 mM concentration, in addition to 2 mM $Pb(NO_3)_2$, 5 mM $MnCl_2$, 2 mM $MgCl_2$, 50 mM TRIS-maleate, 3% dextran T250, and 0.25 M sucrose (pH 7.4). TMS-buffered substrate solution without substrate served as a control. After thorough washing and subsequent color development (1% (v/v) $(NH4)_2S$), a brown deposit of the enzyme reaction product became visible. The sections were dehydrated in graded ethanol (70, 95, and 100% EtOH, and 100% xylol) and mounted with Eukitt (Sigma-Aldrich, St. Louis, MO, USA). The sections were examined and photographed using Leica microscope (Leica Microsystems, Germany). Application of alkaline phosphatase inhibitor levamisole produced no significant effect on the histochemical staining. Cell types and anatomical structures (fiber tracts, blood vessels, and cell types) have been identified on the basis of their morphological appearance.

Relative intensity of histochemical reaction was rated using arbitrary intensity scale, denoting very strong (++++), strong (+++), medium (++), weak (+), and absent (−) reaction.

Preparation of Synaptosome and Gliosome Fractions

Purified hippocampal synaptosome (SYN) and gliosome (GLIO) preparations were isolated by differential centrifugation in discontinuous Percoll gradient, by strictly adhering to the well-established protocol described earlier [40, 46, 47, 51]. Hippocampi were dissected bilaterally and pooled (3/group), homogenized in 10 volumes of ice-cold isolation buffer (0.32 M sucrose, 5 mM Tris-HCl, pH 7.4). Crude nuclear fraction and cell debris were removed by centrifugation at 1000×g for 10 min. Supernatants were collected and centrifuged at 15000×g for 20 min in order to obtain crude membrane fraction (P2). P2 fractions were re-suspended in the isolation buffer, placed on a discontinuous Percoll gradient (2, 6, 10, and 23% v/v Percoll in 0.32 M Tris-buffered sucrose and 1 mM EDTA, pH 7.4), and centrifuged at 35.000×g for 5 min. The bands containing gliosomal and synaptosomal fractions were removed from 2 to 6%, and 10–23% Percoll interface, respectively, diluted in the isolation buffer and washed two times by centrifugation at 12.000×g for 15 min at 4 °C. The Percoll gradient enables efficient separation of SYN from GLIO, since the phases which contain the fractions are clearly separated. GLIO is enriched in astroglial membrane fragments, with negligible neuronal contamination and complete lack of microglia and oligodendrocytes [51, 52]. SYN is highly enriched in enclosed presynaptic and postsynaptic membrane fragments [53]. The purity of the subcellular

preparations was tested by immunoblotting using specific molecular markers for each fraction.

The protein content of the isolated subcellular fractions was determined by using bovine serum albumin (BSA) as a standard, as described previously [44]. For functional assays, samples were used immediately after isolation, while for the immunoblotting procedures, samples were kept at − 80 °C until use.

Hippocampal Primary Astrocyte Culture

One- to 2-day-old rat female pups of the Wistar strain from the local colony were used for primary cortical astrocyte culture preparation. The cerebral hemispheres were isolated, the pial membrane was thoroughly removed, and hippocampi were dissected on ice. The tissue was mechanically dissociated by gentle pipetting under sterile conditions in Leibovitz's L-15 isolating medium supplemented with 2 mM L-glutamine, 100 IU/ml penicillin, 0.1 mg/ml streptomycin, and 0.1% BSA. After two centrifuge/washing steps at 500×*g* for 4 min, cells suspension was passed through ø 0.8- and ø 0.6-mm sterile needles, to remove residual tissue aggregates. Additional centrifugation step at 500×*g* for 4 min was followed by cells resuspension in Dulbecco's modified Eagle's medium with the addition of 10% heat-inactivated fetal bovine serum (FBS), 25 mmol/l glucose, 2 mmol/l L-glutamine, 1 mmol/l sodium pyruvate, 100 IU/ml penicillin, and 100 μg/ml streptomycin. Cells were subsequently seeded in tissue culture flasks for adherent cells and grown at 37 °C in a humified incubator with 5% CO2/95% air. Culture medium was replaced 1 day after the isolation and then every other day until cultures were 80–90% confluent. Primary microglia and oligodendrocytes were removed by mechanical washing using the 1-ml pipette. Adherent primary astrocytes were washed with PBS, trypsinized (0.25% trypsin and 0.02% EDTA) and re-plated on new dishes at a density of 1.5×10^4 cells/cm^2 and maintained to reach confluence. The cell culture was prepared from hippocampal tissue pooled from three female pups.

Gene Expression Analysis by RT-qPCR

The total RNA from the whole hippocampal formation or primary culture was extracted using TRIzol Reagent (Invitrogen, Carlsbad, CA, USA), according to the manufacturer's instructions. The concentration and the purity of the RNA were assessed using OD260 and OD260/OD280 ratio, respectively. The cDNAs were reverse transcribed using High-Capacity cDNA Reverse Transcription Kit (ThermoFisher Scientific, Waltham, MA, USA), according to manufacturer's instructions. The cDNAs were stored at − 20°C until further use. Quantitative real-time PCR was performed using EvaGreen qPCR Mastermix (Applied Biological Materials Inc. Richmond, BC. Canada) and ABI Prism 7000 Sequence Detection System (Applied Biosystems, USA) under the following conditions: 10 min of enzyme activation at 95 °C, 40 cycles of 15-s denaturation at 95 °C, 30-s annealing at 60 °C, 30-s amplification at 72 °C, and 5-s fluorescence measurement at 72 °C. Primer sequences used for the amplification are given in Table 1. The abundance of transcripts was expressed relatively to reference gene, cyclophilin A (CycA) which was used for in vivo analysis, and glyceraldehyde 3-phosphate dehydrogenase (GAPDH) for the treatment in vitro. Relative quantification was performed using the ΔCt method, which results in ratios between target genes and a reference gene. Samples obtained from five animals for each experimental group were run in duplicate. In each run, internal standard curves were generated by several fold dilutions of generated cDNA to check amplification efficacy. Melt curve analysis was performed at the end of every experiment to confirm the formation of a single PCR product.

Functional Ectonucleotidase Assays

The NTPDase and eN activities were evaluated by measuring the formation of inorganic phosphate upon addition of ATP, ADP, or AMP to hippocampal synaptosome or gliosome preparations. Briefly, an aliquot of synaptosome or gliosome fraction containing 10 μg of total proteins was resuspended in assay buffer; preincubated for 10 min at 37 °C; and incubated with the 1-mM ATP, ADP for 10 min, or 1-mM AMP for 30 min, at 37 °C. The level of inorganic phosphates liberated by enzyme actions was determined by the Malachite green method, as described previously [46, 47]. The conditions for the enzyme analyses were chosen in separate experiments in order to ensure linearity of the reactions. The samples from six separate measurements from three independent preparations were run in triplicate, and the activity of each sample was expressed as mean ± SEM (in nmol Pi/mg protein/min). The effects of E2 administration was compared to OVX group, since injection of DMSO produced no apparent influence on the ectonucleotidase activities (data not shown).

Immunoblotting

The expression levels of individual ectonucleotidases were determined by immunoblot analysis [40, 46, 47]. Briefly, equivalent amounts (40 μg of total proteins) were resolved by SDS-PAGE (4–8%) and transferred onto PVDF support membranes (0.45 mm, Millipore, Germany). After washing in TBST (50 mM Tris-HCl pH 7.4, 150 mM NaCl, 0.05% Tween 20), the membranes were blocked in 5% BSA in TBST for 1 h. The membranes were incubated with guinea pig anti-rat NTPDase1 antibodies (1:1000 dilution; ab66215, Abcam, UK), rabbit anti-rat NTPDase2 and NTPDase3 antibodies (1:1000 and 1:2000 dilutions, respectively; clone KLH5 and KLH14, kindly gift from Dr. T.L. Kirley,

Table 1 Primer sequences used for qRT-PCR

Target gene	Forward	Reverse
NTPDase1	TCAAGGACCCGTGCTTTTAC	TCTGGTGGCACTGTTCGTAG
NTPDase2	TGCTTCGACACAGATCACCT	GAATCTGGTCTCGGCCATAG
NTPDase3	GCCTCCACCCAGATATCCTT	CCGTAGCACTGGAAACTGTG
eN	CAAATCTGCCTCTGGAAAGC	ACCTTCCAGAAGGACCCTGT
CycA	CAAAGTTCCAAAGACAGCAGAAAA	CCACCCTGGCACATGAAT
GAPDH	TGGACCTCATGGCCTACAT	GGATGGAATTGTGAGGGAGA

University of Cincinnati, OH, USA), and rabbit anti-rat CD73 (1:2000 dilution; mAb#13160, Cell Signaling, USA), overnight at 4 °C. After washing with TBST, membranes were incubated with appropriate secondary antibodies conjugated to horseradish peroxidase (1:10000 dilution; Santa Cruz Biotechnology, Inc., CA, USA). Support membranes were re-probed with goat anti-rat β-actin antibody (1:250 dilution; sc-1615, Santa Cruz Biotechnology, Inc., CA USA), after visualization of the target protein. Visualization of the bands was performed on X-ray films (AGFA HealthCare NV, Septestraat, Mortsel, Belgium) with the use of chemiluminescence (Immobilon Western Chemiluminescent HRP substrate, Millipore, Darmstadt, Germany). Densitometric analysis was performed using *ImageJ* software package while optical density of each investigated protein band was normalized to appropriate optical density obtained for β-actin. The densitometric data obtained from six separate support membranes obtained with three independently isolated set of samples were averaged and represented as mean ± SEM, relative to the ratio obtained in intact control (arbitrarily defined as 1.0).

Data Analysis

Results of enzyme assays are presented as mean ± SEM, from six separate determinations performed in triplicate. The results of densitometric analysis were presented as mean ± SEM from $n = 6$ separate determinations. Since the differences between OVX and DMSO group were insignificant, the comparisons were made with respect to Intact or OVX group. Data were analyzed with a one-way ANOVA followed by Tukey's multiple-comparison post hoc test using Origin 8.0 software package. The values of $p < 0.05$ or less were considered statistically significant.

Results

Enzyme Histochemistry Reveals Expression and Spatial Distribution of Nucleotide-Hydrolyzing Enzymes Following OVX and E2 Treatment

Spatial distribution of nucleotide-hydrolyzing activities and alterations in their expression induced by OVX and E2 treatment were determined by enzyme histochemistry, using ATP, ADP, and AMP as substrates (Fig.1). Briefly, the addition of individual nucleotides in the presence of lead nitrate results in a precipitation of the reaction product at the site of the respective ectonucleotidase reaction.

ATPase Histochemistry Substantial deposition of the lead phosphate precipitates in the presence of ATP has been observed in intact control (Table 2). Strong histochemical reaction was observed in the superficial layer of CA1-CA2, stratum oriens (so). Equally strong reaction was obtained in CA1-CA2 molecular layer, particularly in stratum radiatum (sr) and stratum moleculare (sm), while the strongest histochemical reaction was obtained in the interposed stratum lacunosum moleculare (slm) (Fig. 1a). Staining intensities in the corresponding layers of CA3 were notably weaker, with faintly stained stratum lucidum (sl). In the dentate gyrus (DG), weaker reaction was obtained in the hilus and subgranular zone (sz). It is of note that the pyramidal cell layer in CA1-CA3 fields and the granular cell layer in the dentate gyrus were completely free of the reaction product. Removal of ovaries (OVX) resulted in reduced histochemical reaction throughout the hippocampus (Fig. 1d) and particularly in layers strongly labeled in intact animals, *slm* and *so*, while E2 treatment resulted in the recovery of ATP-hydrolyzing activity and the staining intensity to a level comparable to intact control (Fig. 1g), in all layers, with the exception of *slm*, which remained slightly light-colored in comparison to intact controls. Microglia and blood vessels were strongly stained in the presence of ATP as a substrate. Alteration in microglia morphology and staining are shown in Supplementary Fig. 1.

ADPase Histochemistry When ADP was applied as a substrate, the pattern of the histochemical staining was notably less intense than that for ATP (Fig. 1b). As expected for the distribution of NTPDase1, which hydrolyzes ATP and ADP almost equally well [27, 28], microglia and blood vessels were depicted by ADPase histochemistry and accounted for much of the staining in the sections, with a faint background staining of the neuropil. Difference in ADPase and ATPase staining indicate that the most of the histochemical reaction observed in the presence of ATP came from NTPDase2, which preferentially hydrolyses ATP [54]. Selective ADPase reaction (not

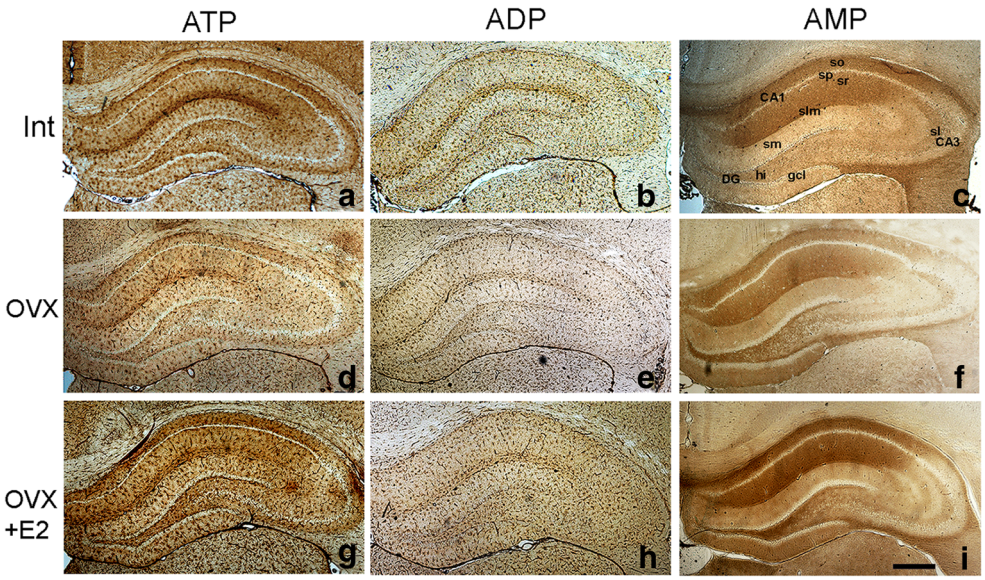

Fig. 1 Distribution of ectonucleotidases in the hippocampal region. Ectonucleotidase histochemistry in the presence of ATP (**a**, **d**, **g**), ADP (**b**, **e**, **h**), and AMP (**c**, **f**, **i**), in hippocampal region of intact control (Int), ovariectomized animals (OVX), and the animals treated with E2 (OVX + E2). **c** Abbreviations indicate the position of hippocampal layers—Cornu Amonis (CA), stratum oriens (so), pyramidal cell layer (sp), stratum radiatum (sr), stratum lacunosum moleculare (slm), stratum lucidum (sl), stratum moleculare (sm), granule cell layer of dentate gyrus (gcl), hilus (hi), and dentate gyrus (DG). **i** Scale bar = 500 μm

obtained in the presence of ATP) has been observed in scattered cells in the granule cell layer in DG. The staining delineated glial cell processes which traversed the pyramidal and DG cell layers. In OVX animals, the ADPase staining intensity became weaker than in intact controls (Fig. 1e), whereas treatment with E2 increased the staining intensity, without apparent changes in the general pattern (Fig. 1h).

AMPase Histochemistry When AMP was applied as a substrate, the pattern of the histochemical reaction clearly differed from those obtained with ATP and ADP, and for the most part, could not be assigned to individual cell types (Fig. 1c). In intact control, the strongest deposition of the reaction product was observed in the superficial layer of CA1-CA2, *so* and *sr*, in the molecular layer and *slm*, while apparently less intense reaction was obtained in *sm*. The moderate reaction was also observed in stratum lucidum (sl) and the hilus of the DG. Other CA3 and DG layers were faintly stained. Again, the pyramidal cells layer of CA1-CA3 and granular cell layer were completely spared. Following OVX, the intensity of

Table 2 Enzyme histochemistry

	ATPase			ADPase			AMPase		
Hippocampal layer	Intact	OVX	OVX + E2	Intact	OVX	E2	Intact	OVX	OVX + E2
CA1									
Stratum oriens	+++	+	++	−/+	–	−/+	++++	+++	++++
Stratum pyramidale	–	–	–	–	–	–	–	–	–
Stratum radiatum	++	+	++	−/+	–	−/+	++++	+++	++++
Stratum lacunosum	++++	++	+++	++	+	+/++	++++	+++	++++
Stratum moleculare	++	+	++	−/+	–	−/+	++++	+++	+++
CA3									
Stratum oriens	++	+	++/+++	+	–	+	+++	−/+	+
Stratum pyramidale	–	–	–	–	–	–	–	–	–
Stratum lucidum	++	+	++	−/+	–	−/+	+++	++	++
Stratum radiatum	++	+	++	−/+	–	−/+	++	−/+	+
Dentate gyrus									
Molecular layer	++	+	+/++	−/+	−/+	−/+	++	+	+
Granular layer	–	–	–	–	–	–	–	–	–
Polymorphic layer	++	+	++	–	+	–	++	+++	++++
Subgranular zone	+++	+	++	–	+	–	++	+++	++++

++++ very strong, +++ strong, ++ medium, + weak, − absent reaction

AMPase reaction notably decreased throughout the hippocampus (Fig. 1f). Here again, treatment with E2 resulted in enhanced staining, particularly in the synaptic regions of CA1, in the subgranular layer of hilus, while neuronal cell layers remained completely unlabeled (Fig. 1i).

Changes in Ectonucleotidase Gene Expression Following OVX and E2 Treatment

RT-qPCR was applied to determine ectonucleotidase gene expression in whole hippocampal tissue following OVX and E2 treatment. The changes in the expression levels of the target genes in each experimental group were expressed relatively to CycA as a reference gene, which enabled comparison of the relative transcript abundance for each gene in each sample. Based on the obtained results, it was deduced that NTPDase2 was the most represented ectonucleotidase in the hippocampal tissue (Fig. 2), being fivefold more abundant than NTPDase1 and 10-fold more abundant than NTPDase3.

In regard to NTPDase1-mRNA abundance (Fig. 2), removal of ovaries induced slight decrease [76.7 ± 25.2%; $F = 1.68$; $p = 0.21$], while E2 treatment induced a modest increase [127.4 ± 35.8%; $F = 1.32$; $p = 0.266$] in respect to intact control, although the changes were not statistically significant. However, comparison of the means between OVX and E2 revealed statistical significance regarding NTPDase1-mRNA abundances [$F = 6.822$; $p = 0.017$].

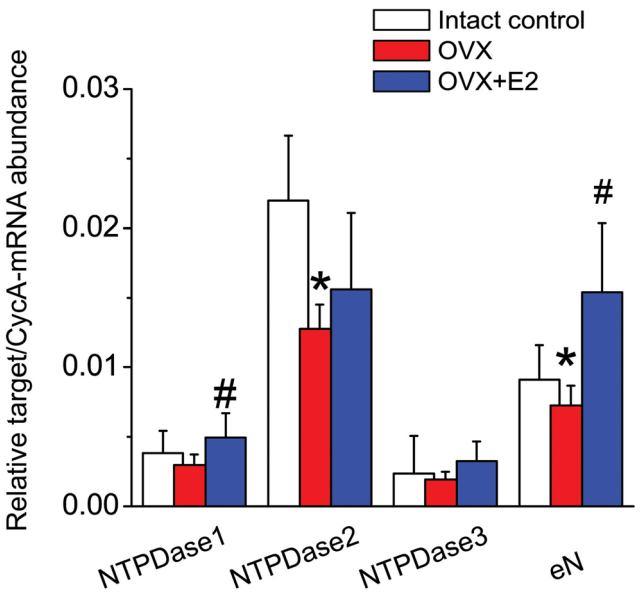

Fig. 2 Ectonucleotidase gene expression in the hippocampal region. The abundance of mRNAs coding for NTPDase1-3 and eN were determined by RT-qPCR in the hippocampal tissue isolated from Int, OVX, and OVX + E2 animals. The abundance of each transcript was expressed relative to CycA as an internal control, and changes in the expression were presented relatively to Int control (100%). Bars represent mean relative mRNA target/CycA gene abundance ± SD, obtained from five animals per experimental group (1 brain/group/isolation). Significance shown inside the graphs: $^{*}p < 0.05$ or less in respect to Int; $^{\#}p < 0.05$ or less in respect to OVX

The most pronounced changes were observed in relation to NTPDase2 gene expression. In OVX animals, the abundance of NTPDase2-mRNA decreased to about half in respect to intact control [58.0 ± 13.8%; $F = 16.64$; $p < 0.001$], whereas the expression increased following E2 treatment to the level comparable with intact control [71.0 ± 35.1%; $F = 3.38$, $p = 0.08$].

OVX and E2 affected the hippocampal expression of eN gene. The abundance of eN-mRNA decreased in OVX group in respect to intact control [79.7 ± 19.7%; $F = 45.37$, $p <<< 0.001$], while E2 treatment induced significant upregulation of the gene and significant increase in eN-mRNA abundance in respect to OVX group [$F = 10.54$; $p = 0.005$].

Accordingly with our previous report [40], the expression levels of NTPDase3-mRNA in the hippocampal tissue did not vary with the treatments.

Expression Analyses of Ectonucleotidases in SYN and GLIO Following OVX and E2 Treatment

The enzyme histochemistry demonstrated that the highest nucleotide-hydrolyzing activities and most pronounced changes in the staining intensities after OVX and E2 were associated with the synapse-rich hippocampal layers, while the neuron-rich layers were almost completely devoid of the histochemical reaction. Therefore, the next set of measurements was conducted on purified subcellular fractions enriched in presynaptic and postsynaptic membranes (SYN) and astrocyte membranes (GLIO).

The levels of ATP and ADP hydrolyses decreased slightly, but significantly in SYN following OVX (Fig. 3a) and were completely restored to the control level after E2 treatment. The values of ATPase/ADPase ratios (Table 3) suggest a heterogeneous distribution of the E-NTPDase family members in SYN. The result of immunoblot analysis corroborated the assumption as it demonstrated that OVX decreased, while E2 positively regulates the expression of NTPDase1 and NTPDase2 in the SYN (Fig. 3b), without change in NTPDase3 protein abundance (data not shown). With regard to AMP hydrolysis, the activity decreased after OVX and recovered to the control level after E2 (Fig. 3a). Immunoblot analysis showed that variations in AMP-hydrolyzing activities were not paralleled with consistent changes in eN protein abundance. Specifically, the decrease in AMPase activity induced by OVX was not accompanied by altered eN protein expression (Fig. 3b, c).

GLIO exhibited a different pattern of nucleotide-hydrolyzing activities in respect to SYN (Fig. 4a–c). While overall levels of ATP and AMP-hydrolyzing activities were similar in two fractions isolated from intact hippocampus, the level of ADP-hydrolyzing activity in GLIO was significantly lower and

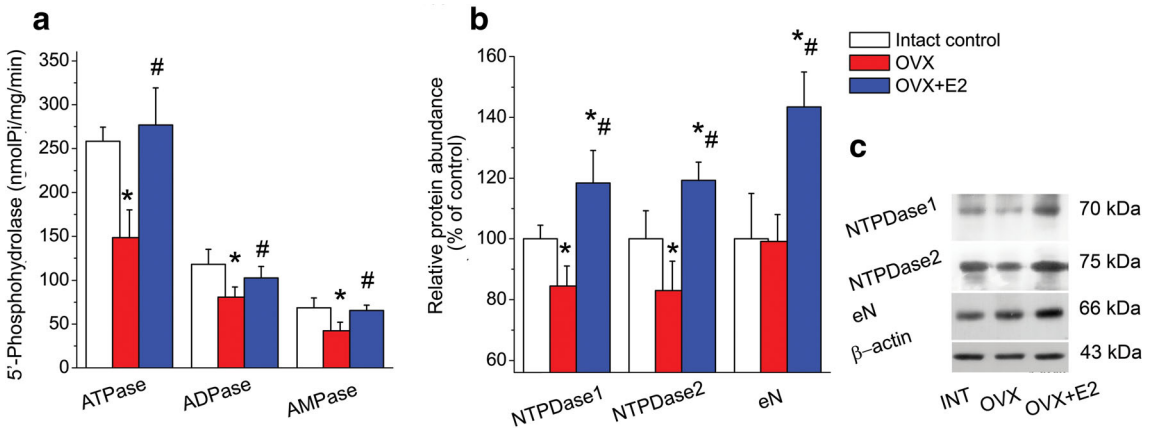

Fig. 3 Expression and functional activity of ectonucleotidases in the hippocampal synaptosomes after ovariectomy and E2 treatment. **a** Levels of 5′-phosphohydrolase activity in presence of ATP, ADP, and AMP, assessed by determining the level of free inorganic phosphate (Pi) in the reaction medium. Bars represent mean 5′-phosphohydrolase activity (nmol Pi/mg/min) ± SEM from at least six separate determinations performed in triplicate, from three independent synaptosome preparations (2–3 brains/group/isolation). **b** Ectonucleotidase protein expression. Bars represent mean protein abundance relative to β-actin ± SEM, from $n > 6$ separate determinations from three separate isolations (2–3 brains/group/isolation). Significance shown inside the graphs: $^{*}p < 0.05$ or less in respect to control; $^{\#}p < 0.05$ or less in respect to OVX

without alteration after the treatments (Fig. 4a, Table 3). Low ADPase activity and the value of ATPase/ADPase of ~ 5 pointed to NTPDase2 as dominant NTPDase in GLIO in control conditions (e.g., cultured astrocytes display ATP/ADP-hydrolyzing ratio of > 10–5:1 [28, 36, 55]). This was confirmed by immunoblot analysis which showed the GLIO is highly enriched in NTPDase2 protein, very faint NTPDase1 (Fig. 4c), and completely free of NTPDase3 bands (data not shown), also shown previously [40]. Recovery of ATP hydrolysis to the control level after E2, without change in ADP hydrolysis (Fig. 4a, Table 3) and upregulation of NTPDase2 protein level (Fig. 5b, c) were observed. OVX reduced the rate of AMP hydrolysis, which is indicative of eN activity, while E2 failed to restore the activity to the control level (Fig. 4a). The decrease in AMP-hydrolyzing activity, however, was not accompanied by a corresponding decrease in protein abundance (Fig. 4c).

Effect of E2 on the Expression of Ectonucleotidases by Primary Hippocampal Astrocytes In Vitro

The results obtained on the purified subcellular fractions suggested that the effects of OVX and E2 in SYN fraction were regulated on transcriptional level, whereas the effects of the treatments in GLIO induced a non-genomic mode of action. To validate the assumption, next measurements were performed in vitro, on primary hippocampal astrocytes isolated from neonatal female rats. The primary astrocyte culture was treated with E2 (1, 5, 10, 25, 50, and 100 nM), for 1, 4, or 24 h, and the abundance of the transcripts coding for NTPDase2 and eN were determined by RT-qPCR (Fig.5). Transient upregulation of NTPDase2 was observed 4 h after the E2 treatment, in the presence of 5–50 nM E2 (Fig. 5a). The maximum effect was observed with 50 nM E2 which induced almost twofold increase in NTPDase2-mRNA abundance. On the other hand, only modest upregulation of eN-mRNA was induced 4 h after the treatment with 5 nM E2 (Fig. 5b).

Discussion

Studies of numerous clinical and experimental CNS disorders show that ovarian hormone estradiol (E2) exhibits strong neuroprotective and neurotrophic effects [16–20]. E2 activates different protective mechanisms in neurons, but also in glial

Table 3 Specific ectonucleotidase activity in the presence of ATP, ADP, and AMP

	SYNAPTOSOMES			GLIOSOMES		
Nucleotide hydrolysis (nmol Pi/mg/min)	Intact	OVX	OVX + E2	Intact	OVX	OVX + E2
ATP	258.2 ± 4.7	148.5 ± 10.8*	276.8 ± 14.3$^{\#}$	211.5 ± 10.6	153.8 ± 7.6*	217.3 ± 12.3$^{\#}$
ADP	119.1 ± 5.4	80.3 ± 5.8*	101.5 ± 4.3$^{\#}$	42.3 ± 3.4	38.7 ± 2.9	39.6 ± 3.3
AMP	68.7 ± 2.7	42.3 ± 3.0*	65.6 ± 2.1$^{\#}$	67.3 ± 2.8	48.2 ± 2.6*	47.2 ± 2.2$^{\#}$
ATPase/ADPase ratio	2.2 ± 0.1	1.8 ± 0.1	2.7 ± 0.1	5.0 ± 0.2	3.9 ± 0.1	5.5 ± 0.2

Significance level: $^{*}p < 0.05$ or less in respect to Intact; $^{\#}p < 0.05$ or less in respect to OVX

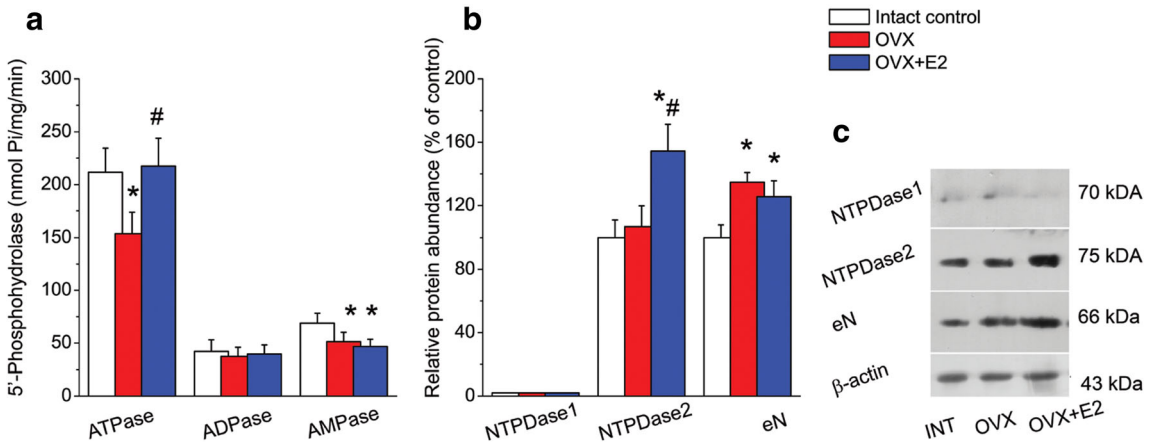

Fig. 4 Expression and functional activity of ectonucleotidases in the hippocampal gliosomes after ovariectomy and E2 treatment. **a** Levels of 5′-phosphohydrolase activity in presence of ATP, ADP, and AMP, assessed by determining the level of free inorganic phosphate (Pi). Bars represent mean specific activity (nmol Pi/mg/min) ± SEM from $n > 6$ separate determinations performed in triplicate, from three separate gliosome preparations (2–3 brains/group/isolation). (**b**) Ectonucleotidase protein expression. Bars represent mean protein abundance relative to β-actin ± SEM, from $n > 6$ separate determinations from three separate isolations (2–3 brains/group/isolation). Significance shown inside the graphs: $^{*}p < 0.05$ or less in respect to control; $^{\#}p < 0.05$ or less in respect to OVX

cells, which have an essential role in the maintenance of brain homeostasis. Among many other signaling events, E2 affects purinergic signaling components [47, 50], which determine duration and extent of extracellular ATP and adenosine actions. Thus, in the present study, we have examined the effect of OVX and estradiol replacement (OVX + E2) on the expression and activity of whole enzyme chain for extracellular nucleotide metabolism in the hippocampus of female rats. In addition, the aim was to identify cell types which are targets of the OVX- and E2-induced effects in the hippocampus.

Spatial distribution of ectonucleotidase enzymes in the hippocampus was examined by enzyme histochemistry, and data obtained for intact control were in line with the existing literature [29]. Briefly, our study confirms that the nucleotide-hydrolyzing activities are mostly localized in synapse-rich hippocampal layers, particularly *so*, *sr*, and *sl*, whereas pyramidal cell layer in CA1-CA3 and granular cell layer of DG are practically reaction-free for all substrates. Also, notably stronger reactions obtained with ATP than with ADP point to NTPDase2 as dominant ectonucleotidase in intact hippocampus. This assumption was supported with the expression analysis data showing that NTPDase2-mRNA was, by far, the most abundant ectonucleotidase transcript expressed in the hippocampal tissue. Our study provides novel data showing that OVX markedly reduces ATPase, ADPase, and AMPase histochemical reactions, whereas E2 restores the histochemical reactions to the level of control. These findings are again supported by expression analysis data showing that OVX downregulates expression of NTPDase1-, NTPDase2-, and eN-mRNA, while E2 restores NTPDase2-mRNA and upregulates NTPDase1- and eN-mRNA significantly above the control level. In addition, it is known that decline of NTPDase1 and eN or both cause a reduction in the length of processes and branching frequency of the microglia [56], as

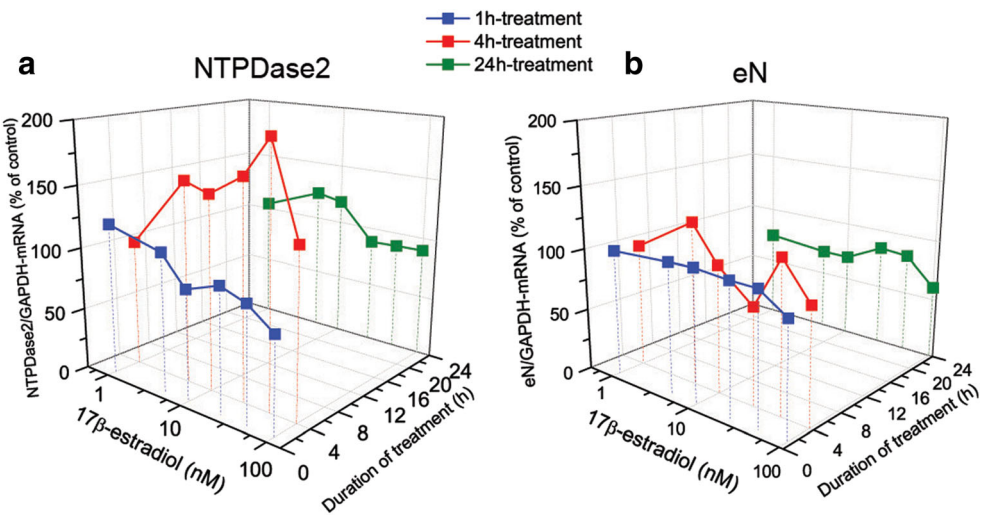

Fig. 5 Expression of ectonucleotidase genes in hippocampal astrocyte cultures following treatment with E2. Confluent astrocyte monolayers were treated with 1–100 nM E2. The cells were harvested 1 to 24 h following the treatment. cDNA was generated from total RNA, and specific target sequences were amplified by RT-qPCR. The transcript abundances were expressed relatively to the abundance of GAPDH-mRNA. Bars represent mean target gene/GAPDH-mRNA abundance ± SEM from one determination performed in duplicate

we observed after OVX. Potentially, elevation of extracellular adenosine production by increased degradation of ATP/ADP/AMP after E2 application enhanced ramification of microglia, presenting typically healthy cells.

Combined immunoblot and enzyme assay data obtained on hippocampal synaptosome- (SYN) and gliosome (GLIO)-enriched fractions led us to three major conclusions. First, investigated subcellular fractions express different combinations of ectonucleotidases. Specifically, SYN expresses NTPDase1/NTPDase2/NTPDase3/eN, while GLIO expresses NTPDase2/eN as dominant ectonucleotidases, which probably results in different basal levels of ATP, ADP, and adenosine in physiological conditions. As we shown previously [40], NTPDase3 is unaltered by hormonal manipulations. Second, the mechanisms of OVX and E2 actions are different in two fractions; In neuronal SYN compartment, OVX and E2 alter expression of ectonucleotidases on genomic level, while in GLIO, the mechanisms include both genomic and non-genomic mode of action. Particularly, in GLIO fraction, changes in NTPDase2 and eN activity occur without apparent change in the protein abundances. Reason might be the existence of different splice variants of NTPDase2 which alternative coding of the intracellular C-terminal domain contributes to distinctive phenotypic variation with respect to extracellular nucleotide specificity, hydrolysis kinetics, and protein trafficking [57–59]. Also, the lack of correlation between changes in eN activity and the protein abundance has been observed previously in different physiological and pathological conditions [41, 44, 46–49].

The classic paradigm of E2 action involves cytosolic estradiol receptors (ERα and β), which bind to proximal estrogen responsive elements (EREs) and, subsequently, regulate expression of target genes. It is of note that promoter regions of neither of ectonucleotidase genes comprise the regulatory ERE element [60, 61]. However, ERα may activate multiple signaling pathways and may induce alternative transcription factors [17, 62, 63], which bind to their specific regulatory elements within the ectonucleotidase genes [64, 65]. Thus, it has been recently demonstrated that E2, acting via ERα, induces transcriptional activation of eN in the hippocampus [47], most likely via activation of AP-1 and Sp1 binding sites present in the core promoter region of *Nt5e* gene [66]. Ultrastructural localization demonstrates that ERs also serve as transducers of E2 actions through non-genomic modes of action. For instance, ERβ is found anchored to lipid rafts and caveolae, physically or functionally coupled to intracellular cascades and second messenger systems which integrate coincident signals from multiple receptors [10]. Besides ERβ [67], NTPDase1, and eN, purinoreceptors and nucleotide transporters are also assembled in lipid rafts [68]. Their reciprocal influences may control duration, magnitude, or direction of responses triggered by multiple signaling systems, and the impact of individual ligands on many short- and long-term functions. Thus, we propose that the outcomes of OVX and E2 observed in present study, which were manifested as discrepancy between the level of an ectonucleotidase activity and the respective protein abundance, were due to non-genomic action and allosteric regulation of the respective enzyme proteins. A high-affinity and functionally relevant interaction between eN and ERβ has been recently documented in hippocampal synaptosomes [47]. The findings obtained in GLIO, which represents only parts of astrocyte cells, were recapitulated and confirmed in vitro, in primary hippocampal astrocyte culture. The in vitro study has demonstrated that E2 upregulates *Entpd2* gene, while affecting *Nt5e* gene expression only slightly. Such results indicated that previously observed effects of E2 on upregulation of eN activity were probably in neurons or mediated at posttranslational level. Given the fact that in vitro, E2 rapidly, within minutes, by binding to membrane estrogen receptors induces activation of different intracellular signaling cascades [8–11], we postulate that E2 induces transient stimulation of *Entpd2* gene expression, which could not be detected 24 h later. Thus, NTPDase2-mRNA upregulation after in vitro E2 exposure could be due to a shift in gene expression levels after their initial and transitory activation by E2.

Since the ectonucleotidase function as an integrated enzyme chain, variations in individual activities impact the enzyme chain as a whole and affect global synaptic activity in the hippocampal formation. For instance, downregulation of NTPDase1/NTPDase2/eN axis, induced by OVX in SYN fraction, may be reflected in situ as a rise in extracellular ATP and an enhancement of fast excitatory P2X-mediated transmission, while downregulation of NTPDase2/eN axis in gliosomes may lead to accumulation of ATP and ADP in the hippocampal parenchyma and potentiation of P2X- and P2Y-mediated responses. It is well-known that ATP and ADP exhibit feed-forward inhibition towards eN [42]. Therefore, it is likely that increased levels of ATP and ADP, due to attenuation of NTPDase1 and 2 activities after OVX, induce feed-forward inhibition of eN, without overall change in the enzyme expression. It can be similarly assumed that E2-induced recovery of NTPDase1/NTPDase2 expression and the upregulation of eN above the control, increase extracellular adenosine levels and enhance A_1R-mediated inhibitory tone in the hippocampus. But, only when extracellular levels of ATP and ADP decrease below the threshold of eN inhibition, adenosine is formed in a considerable amount [42]. All these alterations occur in the specific tissue context in the hippocampus. Based on our data it can be speculated that OVX induces changes that are reflected as an increase in ATP level and potentiation of excitatory transmission on CA1 pyramidal cells, while E2 may lead to an increase in adenosine level and alleviation of the excitatory glutamate actions on CA1 pyramidal cells. Similar alterations in ectonucleotidase activities induced by OVX and E2 were observed in stratum oriens and stratum

radiatum. These two layers comprise septal and commissural fibers and cell bodies of inhibitory interneurons, whose axonal outputs are channeled towards different postsynaptic domains of target pyramidal cells. In this constellation, altered excitability in the inhibitory basket cells due to changes in ATP/adenosine levels may disrupt excitatory-inhibitory balance and affect function of the hippocampal circuits as whole [69].

In conclusion, the steroid hormone-induced alterations in ectonucleotidase activity and/or expression may potentially affect extracellular levels of ATP and adenosine in rat hippocampus, the two signals which shape intrinsic neuronal excitability and function of glial cells. These changes may disturb excitatory-inhibitory synaptic balance and impact on the dynamics of hippocampal circuit. Thus, NTPDase/eN enzyme chain is sensitive to estradiol alteration, and their function probably contributes to plastic events which may be involved in the modulation of cognitive performance after both estrogen decrease, induced by ovary removal, and hormone replacement therapy.

Acknowledgements The authors thank Dr. Terence Kirley from the University of Cincinnati, OH, USA, for a kind gift of rabbit anti-rat NTPDase2 and NTPDase3 antibodies used in this study.

Funding Information The study was entirely supported by Ministry of Education, Science and Technological Development of the Republic of Serbia Nos. OI173044 and III41014.

Compliance with Ethical Standards

All experimental procedures involving rats were approved by the Ethical Committee for the Use of Laboratory Animals of Vinča Institute of Nuclear Sciences, Belgrade, Republic of Serbia (Application No. 02/11) and carried out according to the European Communities Council Directive (2010/63/EU).

Conflict of Interest The authors declare that they have no conflict of interest.

References

1. Prange-Kiel J, Rune GM (2006) Direct and indirect effects of estrogen on rat hippocampus. Neuroscience 138(3):765–772. https://doi.org/10.1016/j.neuroscience.2005.05.061
2. Lisofsky N, Martensson J, Eckert A, Lindenberger U, Gallinat J, Kuhn S (2015) Hippocampal volume and functional connectivity changes during the female menstrual cycle. NeuroImage 118:154–162. https://doi.org/10.1016/j.neuroimage.2015.06.012
3. Woolley CS, McEwen BS (1993) Roles of estradiol and progesterone in regulation of hippocampal dendritic spine density during the estrous cycle in the rat. J Comp Neurol 336(2):293–306. https://doi.org/10.1002/cne.903360210
4. Brinton RD (2009) Estrogen-induced plasticity from cells to circuits: predictions for cognitive function. Trends Pharmacol Sci 30(4):212–222. https://doi.org/10.1016/j.tips.2008.12.006
5. Galea LA, Uban KA, Epp JR, Brummelte S, Barha CK, Wilson WL, Lieblich SE, Pawluski JL (2008) Endocrine regulation of cognition and neuroplasticity: our pursuit to unveil the complex interaction between hormones, the brain, and behaviour. Can J Exp Psychol 62(4):247–260. https://doi.org/10.1037/a0014501
6. Fester L, Prange-Kiel J, Zhou L, Blittersdorf BV, Bohm J, Jarry H, Schumacher M, Rune GM (2012) Estrogen-regulated synaptogenesis in the hippocampus: sexual dimorphism in vivo but not in vitro. J Steroid Biochem Mol Biol 131(1–2):24–29. https://doi.org/10.1016/j.jsbmb.2011.11.010
7. Frankfurt M, Luine V (2015) The evolving role of dendritic spines and memory: interaction(s) with estradiol. Horm Behav 74:28–36. https://doi.org/10.1016/j.yhbeh.2015.05.004
8. Frick KM, Kim J, Tuscher JJ, Fortress AM (2015) Sex steroid hormones matter for learning and memory: estrogenic regulation of hippocampal function in male and female rodents. Learn Mem 22(9):472–493. https://doi.org/10.1101/lm.037267.114
9. Hara Y, Waters EM, McEwen BS, Morrison JH (2015) Estrogen effects on cognitive and synaptic health over the lifecourse. Physiol Rev 95(3):785–807. https://doi.org/10.1152/physrev.00036.2014
10. Sellers K, Raval P, Srivastava DP (2015) Molecular signature of rapid estrogen regulation of synaptic connectivity and cognition. Front Neuroendocrinol 36:72–89. https://doi.org/10.1016/j.yfrne.2014.08.001
11. Phan A, Suschkov S, Molinaro L, Reynolds K, Lymer JM, Bailey CD, Kow LM, MacLusky NJ et al (2015) Rapid increases in immature synapses parallel estrogen-induced hippocampal learning enhancements. Proc Natl Acad Sci U S A 112(52):16018–16023. https://doi.org/10.1073/pnas.1522150112
12. Henderson VW (2008) Cognitive changes after menopause: influence of estrogen. Clin Obstet Gynecol 51(3):618–626. https://doi.org/10.1097/GRF.0b013e318180ba10
13. Krug R, Born J, Rasch B (2006) A 3-day estrogen treatment improves prefrontal cortex-dependent cognitive function in postmenopausal women. Psychoneuroendocrinology 31(8):965–975. https://doi.org/10.1016/j.psyneuen.2006.05.007
14. Habib P, Beyer C (2015) Regulation of brain microglia by female gonadal steroids. J Steroid Biochem Mol Biol 146:3–14. https://doi.org/10.1016/j.jsbmb.2014.02.018
15. Sarvari M, Kallo I, Hrabovszky E, Solymosi N, Liposits Z (2014) Ovariectomy and subsequent treatment with estrogen receptor agonists tune the innate immune system of the hippocampus in middle-aged female rats. PLoS One 9(2):e88540. https://doi.org/10.1371/journal.pone.0088540
16. Acaz-Fonseca E, Avila-Rodriguez M, Garcia-Segura LM, Barreto GE (2016) Regulation of astroglia by gonadal steroid hormones under physiological and pathological conditions. Prog Neurobiol 144:5–26. https://doi.org/10.1016/j.pneurobio.2016.06.002
17. Hamilton RT, Rettberg JR, Mao Z, To J, Zhao L, Appt SE, Register TC, Kaplan JR et al (2011) Hippocampal responsiveness to 17beta-estradiol and equol after long-term ovariectomy: implication for a therapeutic window of opportunity. Brain Res 1379:11–22. https://doi.org/10.1016/j.brainres.2011.01.029
18. Gillies GE, McArthur S (2010) Estrogen actions in the brain and the basis for differential action in men and women: a case for sex-specific medicines. Pharmacol Rev 62(2):155–198. https://doi.org/10.1124/pr.109.002071
19. Potier M, Georges F, Brayda-Bruno L, Ladepeche L, Lamothe V, Al Abed AS, Groc L, Marighetto A (2016) Temporal memory and its enhancement by estradiol requires surface dynamics of hippocampal CA1 N-methyl-D-aspartate receptors. Biol Psychiatry 79(9):735–745. https://doi.org/10.1016/j.biopsych.2015.07.017
20. Stanojlovic M, Gusevac I, Grkovic I, Mitrovic N, Zlatkovic J, Horvat A, Drakulic D (2016) Repeated estradiol treatment attenuates chronic cerebral hypoperfusion-induced neurodegeneration in rat hippocampus. Cell Mol Neurobiol 36(6):989–999. https://doi.org/10.1007/s10571-015-0289-0

21. Sherwin BB (2012) Estrogen and cognitive functioning in women: lessons we have learned. Behav Neurosci 126(1):123–127. https://doi.org/10.1037/a0025539
22. Schipper HM (2016) The impact of gonadal hormones on the expression of human neurological disorders. Neuroendocrinology 103(5):417–431. https://doi.org/10.1159/000440620
23. Burnstock G (2007) Physiology and pathophysiology of purinergic neurotransmission. Physiol Rev 87(2):659–797. https://doi.org/10.1152/physrev.00043.2006
24. Burnstock G (2016) An introduction to the roles of purinergic signalling in neurodegeneration, neuroprotection and neuroregeneration. Neuropharmacology 104:4–17. https://doi.org/10.1016/j.neuropharm.2015.05.031
25. Koles L, Kato E, Hanuska A, Zadori ZS, Al-Khrasani M, Zelles T, Rubini P, Illes P (2016) Modulation of excitatory neurotransmission by neuronal/glial signalling molecules: interplay between purinergic and glutamatergic systems. Purinergic Signal 12(1):1–24. https://doi.org/10.1007/s11302-015-9480-5
26. Sebastiao AM, Ribeiro JA (2015) Neuromodulation and metamodulation by adenosine: impact and subtleties upon synaptic plasticity regulation. Brain Res 1621:102–113. https://doi.org/10.1016/j.brainres.2014.11.008
27. Zimmermann H, Zebisch M, Strater N (2012) Cellular function and molecular structure of ecto-nucleotidases. Purinergic Signal 8(3):437–502. https://doi.org/10.1007/s11302-012-9309-4
28. Robson SC, Sevigny J, Zimmermann H (2006) The E-NTPDase family of ectonucleotidases: structure function relationships and pathophysiological significance. Purinergic Signal 2(2):409–430. https://doi.org/10.1007/s11302-006-9003-5
29. Langer D, Hammer K, Koszalka P, Schrader J, Robson S, Zimmermann H (2008) Distribution of ectonucleotidases in the rodent brain revisited. Cell Tissue Res 334(2):199–217. https://doi.org/10.1007/s00441-008-0681-x
30. Grkovic I, Drakulic D, Martinovic J, Mitrovic N (2017) Role of ectonucleotidases in the synapse formation during brain development: physiological and pathological implications. Curr Neuropharmacol 15. https://doi.org/10.2174/1570159X15666170518151541
31. Bjelobaba I, Stojiljkovic M, Pekovic S, Dacic S, Lavrnja I, Stojkov D, Rakic L, Nedeljkovic N (2007) Immunohistological determination of ecto-nucleoside triphosphate diphosphohydrolase1 (NTPDase1) and 5′-nucleotidase in rat hippocampus reveals overlapping distribution. Cell Mol Neurobiol 27(6):731–743. https://doi.org/10.1007/s10571-007-9159-8
32. Wang TF, Guidotti G (1998) Widespread expression of ecto-apyrase (CD39) in the central nervous system. Brain Res 790(1–2):318–322
33. Braun N, Sevigny J, Robson SC, Enjyoji K, Guckelberger O, Hammer K, Di Virgilio F, Zimmermann H (2000) Assignment of ecto-nucleoside triphosphate diphosphohydrolase-1/cd39 expression to microglia and vasculature of the brain. Eur J Neurosci 12(12):4357–4366
34. Brisevac D, Adzic M, Laketa D, Parabucki A, Milosevic M, Lavrnja I, Bjelobaba I, Sevigny J et al (2015) Extracellular ATP selectively upregulates ecto-nucleoside triphosphate diphosphohydrolase 2 and ecto-5'-nucleotidase by rat cortical astrocytes in vitro. J Mol Neurosci 57(3):452–462. https://doi.org/10.1007/s12031-015-0601-y
35. Jakovljevic M, Lavrnja I, Bozic I, Savic D, Bjelobaba I, Pekovic S, Sevigny J, Nedeljkovic N et al (2017) Down-regulation of NTPDase2 and ADP-sensitive P2 purinoceptors correlate with severity of symptoms during experimental autoimmune encephalomyelitis. Front Cell Neurosci 11:333. https://doi.org/10.3389/fncel.2017.00333
36. Wink MR, Braganhol E, Tamajusuku AS, Lenz G, Zerbini LF, Libermann TA, Sevigny J, Battastini AM et al (2006) Nucleoside triphosphate diphosphohydrolase-2 (NTPDase2/CD39L1) is the dominant ectonucleotidase expressed by rat astrocytes. Neuroscience 138(2):421–432. https://doi.org/10.1016/j.neuroscience.2005.11.039
37. Braun N, Sevigny J, Mishra SK, Robson SC, Barth SW, Gerstberger R, Hammer K, Zimmermann H (2003) Expression of the ecto-ATPase NTPDase2 in the germinal zones of the developing and adult rat brain. Eur J Neurosci 17(7):1355–1364
38. Shukla V, Zimmermann H, Wang L, Kettenmann H, Raab S, Hammer K, Sevigny J, Robson SC et al (2005) Functional expression of the ecto-ATPase NTPDase2 and of nucleotide receptors by neuronal progenitor cells in the adult murine hippocampus. J Neurosci Res 80(5):600–610. https://doi.org/10.1002/jnr.20508
39. Belcher SM, Zsarnovszky A, Crawford PA, Hemani H, Spurling L, Kirley TL (2006) Immunolocalization of ecto-nucleoside triphosphate diphosphohydrolase 3 in rat brain: implications for modulation of multiple homeostatic systems including feeding and sleep-wake behaviors. Neuroscience 137(4):1331–1346. https://doi.org/10.1016/j.neuroscience.2005.08.086
40. Grkovic I, Bjelobaba I, Mitrovic N, Lavrnja I, Drakulic D, Martinovic J, Stanojlovic M, Horvat A et al (2016) Expression of ecto-nucleoside triphosphate diphosphohydrolase3 (NTPDase3) in the female rat brain during postnatal development. J Chem Neuroanat 77:10–18. https://doi.org/10.1016/j.jchemneu.2016.04.001
41. Lavrnja I, Laketa D, Savic D, Bozic I, Bjelobaba I, Pekovic S, Nedeljkovic N (2015) Expression of a second ecto-5′-nucleotidase variant besides the usual protein in symptomatic phase of experimental autoimmune encephalomyelitis. J Mol Neurosci 55(4):898–911. https://doi.org/10.1007/s12031-014-0445-x
42. Cunha RA (2001) Regulation of the ecto-nucleotidase pathway in rat hippocampal nerve terminals. Neurochem Res 26(8–9):979–991
43. Kukulski F, Komoszynski M (2003) Purification and characterization of NTPDase1 (ecto-apyrase) and NTPDase2 (ecto-ATPase) from porcine brain cortex synaptosomes. Eur J Biochem 270(16):3447–3454
44. Stanojevic I, Bjelobaba I, Nedeljkovic N, Drakulic D, Petrovic S, Stojiljkovic M, Horvat A (2011) Ontogenetic profile of ecto-5′-nucleotidase in rat brain synaptic plasma membranes. Int J Dev Neurosci 29(4):397–403. https://doi.org/10.1016/j.ijdevneu.2011.03.003
45. Grkovic I, Bjelobaba I, Nedeljkovic N, Mitrovic N, Drakulic D, Stanojlovic M, Horvat A (2014) Developmental increase in ecto-5′-nucleotidase activity overlaps with appearance of two immunologically distinct enzyme isoforms in rat hippocampal synaptic plasma membranes. J Mol Neurosci 54(1):109–118. https://doi.org/10.1007/s12031-014-0256-0
46. Mitrovic N, Zaric M, Drakulic D, Martinovic J, Sevigny J, Stanojlovic M, Nedeljkovic N, Grkovic I (2017) 17beta-estradiol-induced synaptic rearrangements are accompanied by altered ectonucleotidase activities in male rat hippocampal synaptosomes. J Mol Neurosci 61(3):412–422. https://doi.org/10.1007/s12031-016-0877-6
47. Mitrovic N, Zaric M, Drakulic D, Martinovic J, Stanojlovic M, Sevigny J, Horvat A, Nedeljkovic N et al (2016) 17Beta-estradiol upregulates ecto-5′-nucleotidase (CD73) in hippocampal synaptosomes of female rats through action mediated by estrogen receptor-alpha and -beta. Neuroscience 324:286–296. https://doi.org/10.1016/j.neuroscience.2016.03.022
48. Brisevac D, Bjelobaba I, Bajic A, Clarner T, Stojiljkovic M, Beyer C, Andjus P, Kipp M et al (2012) Regulation of ecto-5′-nucleotidase (CD73) in cultured cortical astrocytes by different inflammatory factors. Neurochem Int 61(5):681–688. https://doi.org/10.1016/j.neuint.2012.06.017
49. Da Silva RS, Richetti SK, Tonial EM, Bogo MR, Bonan CD (2012) Profile of nucleotide catabolism and ectonucleotidase expression

from the hippocampi of neonatal rats after caffeine exposure. Neurochem Res 37(1):23–30. https://doi.org/10.1007/s11064-011-0577-0

50. Mitrovic N, Gusevac I, Drakulic D, Stanojlovic M, Zlatkovic J, Sevigny J, Horvat A, Nedeljkovic N et al (2016) Regional and sex-related differences in modulating effects of female sex steroids on ecto-5′-nucleotidase expression in the rat cerebral cortex and hippocampus. Gen Comp Endocrinol 235:100–107. https://doi.org/10.1016/j.ygcen.2016.06.018
51. Milanese M, Bonifacino T, Zappettini S, Usai C, Tacchetti C, Nobile M, Bonanno G (2009) Glutamate release from astrocytic gliosomes under physiological and pathological conditions. Int Rev Neurobiol 85:295–318. https://doi.org/10.1016/S0074-7742(09)85021-6
52. Bari M, Bonifacino T, Milanese M, Spagnuolo P, Zappettini S, Battista N, Giribaldi F, Usai C et al (2011) The endocannabinoid system in rat gliosomes and its role in the modulation of glutamate release. Cell Mol Life Sci 68(5):833–845. https://doi.org/10.1007/s00018-010-0494-4
53. Corera AT, Doucet G, Fon EA (2009) Long-term potentiation in isolated dendritic spines. PLoS One 4(6):e6021. https://doi.org/10.1371/journal.pone.0006021
54. Heine P, Braun N, Heilbronn A, Zimmermann H (1999) Functional characterization of rat ecto-ATPase and ecto-ATP diphosphohydrolase after heterologous expression in CHO cells. Eur J Biochem 262(1):102–107
55. Wink MR, Braganhol E, Tamajusuku AS, Casali EA, Karl J, Barreto-Chaves ML, Sarkis JJ, Battastini AM (2003) Extracellular adenine nucleotides metabolism in astrocyte cultures from different brain regions. Neurochem Int 43(7):621–628
56. Matyash M, Zabiegalov O, Wendt S, Matyash V, Kettenmann H (2017) The adenosine generating enzymes CD39/CD73 control microglial processes ramification in the mouse brain. PLoS One 12(4):e0175012. https://doi.org/10.1371/journal.pone.0175012
57. Vlajkovic SM, Housley GD, Greenwood D, Thorne PR (1999) Evidence for alternative splicing of ecto-ATPase associated with termination of purinergic transmission. Brain Res Mol Brain Res 73(1–2):85–92
58. Vlajkovic SM, Wang CJ, Soeller C, Zimmermann H, Thorne PR, Housley GD (2007) Activation-dependent trafficking of NTPDase2 in Chinese hamster ovary cells. Int J Biochem Cell Biol 39(4):810–817. https://doi.org/10.1016/j.biocel.2007.01.003
59. Wang CJ, Vlajkovic SM, Housley GD, Braun N, Zimmermann H, Robson SC, Sevigny J, Soeller C et al (2005) C-terminal splicing of NTPDase2 provides distinctive catalytic properties, cellular distribution and enzyme regulation. Biochem J 385(Pt 3):729–736. https://doi.org/10.1042/BJ20040852
60. Hansen KR, Resta R, Webb CF, Thompson LF (1995) Isolation and characterization of the promoter of the human 5′-nucleotidase (CD73)-encoding gene. Gene 167(1–2):307–312
61. Spychala J, Lazarowski E, Ostapkowicz A, Ayscue LH, Jin A, Mitchell BS (2004) Role of estrogen receptor in the regulation of ecto-5′-nucleotidase and adenosine in breast cancer. Clin Cancer Res 10(2):708–717
62. Zelinski DP, Zantek ND, Walker-Daniels J, Peters MA, Taparowsky EJ, Kinch MS (2002) Estrogen and Myc negatively regulate expression of the EphA2 tyrosine kinase. J Cell Biochem 85(4):714–720. https://doi.org/10.1002/jcb.10186
63. Vivar OI, Zhao X, Saunier EF, Griffin C, Mayba OS, Tagliaferri M, Cohen I, Speed TP et al (2010) Estrogen receptor beta binds to and regulates three distinct classes of target genes. J Biol Chem 285(29):22059–22066. https://doi.org/10.1074/jbc.M110.114116
64. Spychala J, Zimmermann AG, Mitchell BS (1999) Tissue-specific regulation of the ecto-5′-nucleotidase promoter. Role of the camp response element site in mediating repression by the upstream regulatory region. J Biol Chem 274(32):22705–22712
65. Carroll JS, Meyer CA, Song J, Li W, Geistlinger TR, Eeckhoute J, Brodsky AS, Keeton EK et al (2006) Genome-wide analysis of estrogen receptor binding sites. Nat Genet 38(11):1289–1297. https://doi.org/10.1038/ng1901
66. Spychala J, Mitchell BS, Barankiewicz J (1997) Adenosine metabolism during phorbol myristate acetate-mediated induction of HL-60 cell differentiation: changes in expression pattern of adenosine kinase, adenosine deaminase, and 5′-nucleotidase. J Immunol 158(10):4947–4952
67. Milner TA, Ayoola K, Drake CT, Herrick SP, Tabori NE, McEwen BS, Warrier S, Alves SE (2005) Ultrastructural localization of estrogen receptor beta immunoreactivity in the rat hippocampal formation. J Comp Neurol 491(2):81–95. https://doi.org/10.1002/cne.20724
68. Bilbao PS, Katz S, Boland R (2012) Interaction of purinergic receptors with GPCRs, ion channels, tyrosine kinase and steroid hormone receptors orchestrates cell function. Purinergic Signal 8(1):91–103. https://doi.org/10.1007/s11302-011-9260-9
69. Campanac E, Gasselin C, Baude A, Rama S, Ankri N, Debanne D (2013) Enhanced intrinsic excitability in basket cells maintains excitatory-inhibitory balance in hippocampal circuits. Neuron 77(4):712–722. https://doi.org/10.1016/j.neuron.2012.12.020